ELSEVIER

Polymer 41 (2000) 4143–4148

polymer

Structure development in poly(ethylene terephthalate) quenched from the melt at high cooling rates: X-ray scattering and microhardness study

F.J. Baltá Calleja[a,*], M.C. García Gutiérrez[a], D.R. Rueda[a], S. Piccarolo[b]

[a]*Instituto de Estructura de la Materia, CSIC, Serrano 119, 28006 Madrid, Spain*
[b]*Dipartimento di Ingegneria Chimica dei Processi e dei Materiali, Università di Palermo, Viale delle Scienze, 90128 Palermo, Italy*

Received 10 August 1999; accepted 2 September 1999

Abstract

The structure and microhardness of poly(ethylene terephthalate) (PET) cooled from the melt, using a wide range of cooling rates, was studied. PET thin films rapidly cooled from the melt (cooling rates larger than 5°C/s) show a continuous variation of structure and properties depending on cooling rate. Results highlight differences in the micro-mechanical properties of the glass suggesting the occurrence of amorphous structures with different degrees of internal chain ordering. The comparative X-ray scattering study of two glassy PET samples (7500 and 17°C/s) reveals the occurrence of frozen-in electron density states giving rise to an excess of scattering for the amorphous sample solidified at a lower cooling rate. The initial glassy structure and its evolution, during isothermal cold crystallization at 117°C of these two samples can be interpreted by assuming an improvement in the state of internal order. The differences in the incipient molecular ordering, which are detected by SAXS but not by WAXS, could be responsible for the hardening observed in the glassy PET samples.

Keywords: Poly(ethylene terephthalate); Solidification under fast cooling; Glassy states

1. Introduction

The study of the crystallization of polymers under fast cooling (at times of the order of tenths of a second) has emerged as a new method of great technological interest [1]. This is so because it allows the control of thermal history and the analysis of crystallization kinetics at high cooling rates [1–5]. A continuous variation of morphology and crystal structure has been shown to be present when varying the cooling rate [3]. In polyolefins, i-polypropylene for instance, at high cooling rates (above 20°C/s) mesomorphic and crystalline phases may coexist with spherulitic morphology surrounded by a weakly birefringent medium. At lower cooling rates only the crystalline monoclinic phase is formed. This competition has been recognized and used to model the crystallization kinetics at high cooling rates by an extension of a non isothermal formulation of the Kolmogoroff–Avrami–Evans (KAE) approach [4,5].

In recent years the investigation of the microhardness (*H*) has appeared as a physical method that can provide quantitative information on changes in the morphology of polymers [6,7]. Specifically, the isothermal crystallization of PET from the glass at different annealing times and temperatures has been followed by microhardness [8]. Microhardness measurements could accurately detect the gradual transition between structures in which spherulitic growth is incomplete, and structures in which such a growth is completed. In the former materials, *H* was shown to be an increasing linear function of the volume fraction of the spherulites. In the latter materials, *H* is nearly constant with annealing temperature [8] but depends on aging conditions [9]. The kinetics of crystallization for PET was also investigated in real time by measuring the variation of *H* "in situ", as a function of time, at different crystallization temperatures [10]. The changes in *H* of injection-molded PET using a range of mold temperatures have also been discussed in the light of the volume fraction of spherulites filling the molds [11].

The aim of the present study is to extend the above investigations to analyze the structure development of thin amorphous-PET films quenched at high cooling rates from the melt. Particularly, we will show that for the higher cooling rates used, glassy PET exhibits an amorphous structure, which is characterized by relatively high hardness values and by a concurrent excess of X-ray scattering intensity at small angles, as compared with conventional amorphous-PET.

* Corresponding author.

0032-3861/00/$ - see front matter
PII: S0032-3861(99)00640-0

Table 1
Density, microhardness and degree of crystallinity of PET solidified from the melt at different cooling rates

Sample	°C/s	ρ (g/cm^3)	H (MPa)	α (%)
1	7500	1.3392	129	3.09
2	700	1.3389	132	2.88
3	178	1.3394	136	3.24
4	88.5	1.3406	140	4.09
5	76.3	1.3408	143	4.24
6	18.7	1.3416	149	4.81
7	17.0	1.3410	143	4.38
8	4.70	1.3439	154	5.73
9	2.30	1.3590	157	17.08
10	1.70	1.3585	157	16.74
11	1.50	1.3610	159	18.48
12	0.60	1.3788	170	30.67
13	0.09	1.4006	174	45.19
14	0.04	1.3953	173	41.71

2. Experimental

2.1. Materials

The material used for this investigation is a standard DMT-based PET with an intrinsic viscosity of 0.62 dl/g, kindly supplied by SINCO Engng, Italy. Before melting the material was dried at 150°C under vacuum for 12 h. Thin films of the material were molten at 280°C for 10 min and then quenched while the cooling history was recorded using a procedure recently described [1–3]. Different cooling conditions can be spanned in this way giving rise to a continuous variation of structure features, from highly crystalline samples to completely amorphous ones (see Table 1). In the case of PET the temperature window determining its solidification has been identified in the vicinity of 170°C, where the maximum of the kinetic constant vs. temperature dependence is found by modeling the crystallization kinetics with the mentioned KAE approach [12].

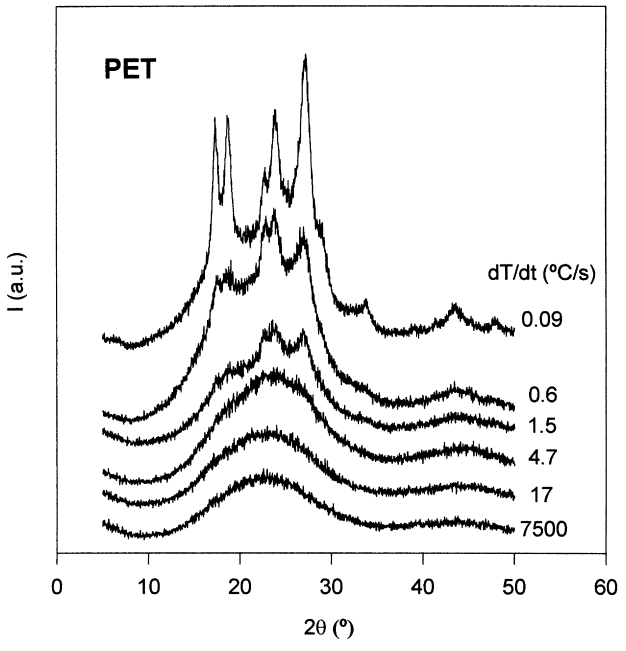

Fig. 1. X-ray diffractograms of thin PET samples cooled from the melt at different cooling rates, dT/dt.

Therefore, the cooling rates measured at this temperature (Table 1) are those used throughout the paper in relation to the developed structure. In order to minimize the aging of the materials after their preparation, the samples were stored in a closed vessel with silica gel (dry atmosphere) inside a freezer.

2.2. Techniques

The density ρ of the samples was measured in a density gradient column containing a mixture of hexane and tetrachloroethane. From the density we have calculated the volume degree of crystallinity α by using the equation $\alpha = \rho_c(\rho - \rho_a)/\rho(\rho_c - \rho_a)$, where the density of the amorphous regions ρ_a was assumed to be 1.3349 g/cm^3 [13] and the density of the crystals ρ_c was taken as 1.4895 g/cm^3 [14].

Microhardness was measured at room temperature using a Leitz "Durimet" tester with a Vickers square pyramidal diamond indenter. The H-value (in MPa) was derived from the residual projected impression using the equation: $H = Kp/d^2$, where d is the mean diagonal length of the indentation in meters, p the applied force in Newtons, and K a geometrical factor equal to 1.854 [15]. Loads of 0.10, 0.15 and 0.25 N to correct for instant elastic recovery were used. A loading cycle of 0.1 min to minimize creep of the material under the indenter was adopted.

The samples were characterized by X-ray diffraction performed at room temperature. A Seifert XRD 3000 θ/θ diffractometer using Ni-filtered CuK_α radiation and a scanning speed of about 1° (2θ)/min were used. In addition, time-resolved measurements of simultaneous, small and wide-angle X-ray scattering (SAXS and WAXS) during isothermal crystallization of two glassy PET samples with different cooling rates were performed at HASYLAB (Hamburg). Synchrotron X-ray radiation, with a wavelength $\lambda = 0.150$ nm, at the polymer beam-line A2 was used. The accumulation time for each X-ray pattern was 30 s.

3. Results and discussion

3.1. X-ray scattering and microhardness studies

Fig. 1 illustrates the changes occurring in the X-ray diffraction pattern of PET quenched from the melt at different cooling rates. With decreasing cooling rate one sees a gradual transformation from the original amorphous halo to the incipient appearance of the crystalline reflections, at about 1.5°C/s. In addition, one observes a continuous increase in the perfection of the crystals as revealed by the sharpening of the X-ray scattering peaks associated to the triclinic crystal phase [14]. The results of Fig. 1 also

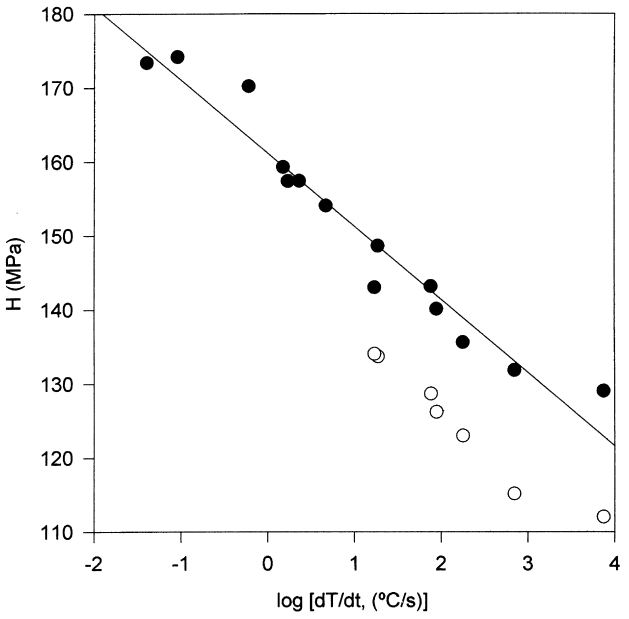

Fig. 2. Plot of H measured at room temperature vs. the logarithm of cooling rate for PET samples: (●) 40 days after their preparation, (○) the same glassy PET samples treated at 95°C for 2 min.

indicate that glassy PET samples are obtained for cooling rates larger than 5°C/s.

The gradual variation in ρ and H-values with cooling rate for the amorphous samples (1–7) suggests the occurrence of changes in the amorphous structure (Table 1).

Fig. 2 illustrates the linear variation of H (measured 40 days after preparation) (filled symbols), vs. the log of cooling rate, dT/dt. It is noteworthy that the lowest H-values observed for the higher cooling rates (amorphous-PET) are larger than those previously reported for glassy PET [8]. The high H-values detected for amorphous-PET in the present study can be attributed to physical aging of the samples. The lower H-values obtained (open symbols) for the same samples measured after 2 min of thermal treatment at 95°C (fresh samples) confirm this assumption [16]. The aged glassy samples show, indeed, distinct higher H-values than the freshly prepared ones. Physical aging below T_g is connected to local molecular motions (conformational changes). In preceding studies we suggested [10] that these changes may involve ordering of benzene rings within PET molecules reducing segmental mobility. Physical aging can be visualized as a densification mechanism [16] below T_g, which results in a hardening of the polymer. It is noteworthy that the amorphous fresh samples still exhibit a large H variation (112–133 MPa), which suggests the occurrence of different structures in the amorphous samples induced during the quenching process from the melt at different cooling rates.

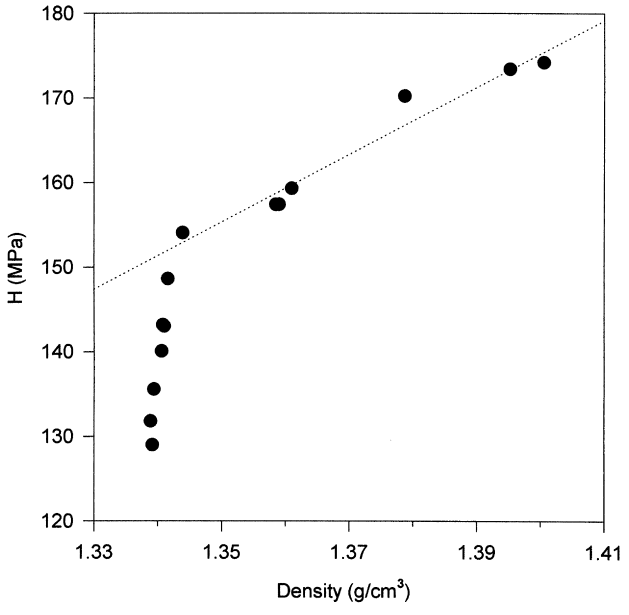

Fig. 3. Plot of H as a function of the macroscopic density of the PET cooled from the melt.

3.2. Structure–microhardness correlation

Fig. 3 illustrates the variation of H for the aged PET samples (Table 1) as a function of macroscopic density. One clearly distinguishes between two regions of behavior: (a) a fast linear increase of H vs. ρ for the amorphous (glassy) samples up to densities of 1.343 g/cm^3 and (b) a second slower linear increase of H vs. ρ for the semicrystalline materials up to $\rho = 1.4$ g/cm^3. In order to discuss the results, we have represented in Fig. 4, the variation of H as a function of the degree of crystallinity, α, derived from density. For the semicrystalline samples (dT/d$t \leq 2.3$°C/s) we confirm the linear variation of H as a function of α, which for $\alpha = 0$, extrapolates to $H = 152$ MPa. However, for the samples crystallized at higher cooling rates with volume degree of crystallinity smaller than 5%, the X-ray diffraction pattern does not show any crystalline peaks (Fig. 1). What could, then, be the reason for such a steep variation of H (from 129 up to 145 MPa) in these samples which do not exhibit any X-ray crystallinity? One possible explanation for the relatively high H-values of the glassy samples could be given in light of emerging local regions with different degrees of internal order which may become precursors of final crystalline states. Hence, it appears that different high cooling rates may give rise to glassy PET with H-values which could be connected to embryonic regions of higher density which, however, do not give rise to any WAXS signal. Embryonic chain ordering prior to isothermal crystallization from the glass has been reported for glassy PET [17] and poly(ether-ketone-ketone) [18] samples in which the SAXS maximum develops, during isothermal treatment, before the appearance of the WAXS crystalline peaks. Prenucleation density fluctuations have been proposed to be responsible for the ordering phenomena during the induction period, before cold crystallization in PET [17], as well as, prior to melt crystallization

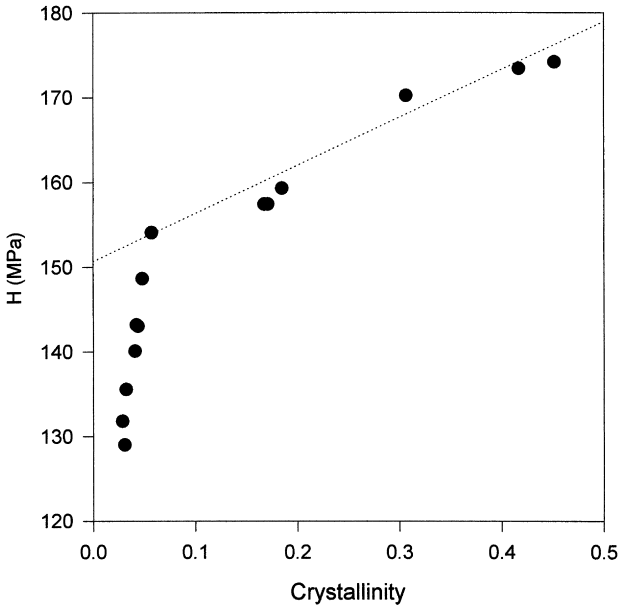

Fig. 4. Microhardness dependence on degree of crystallinity α calculated from density.

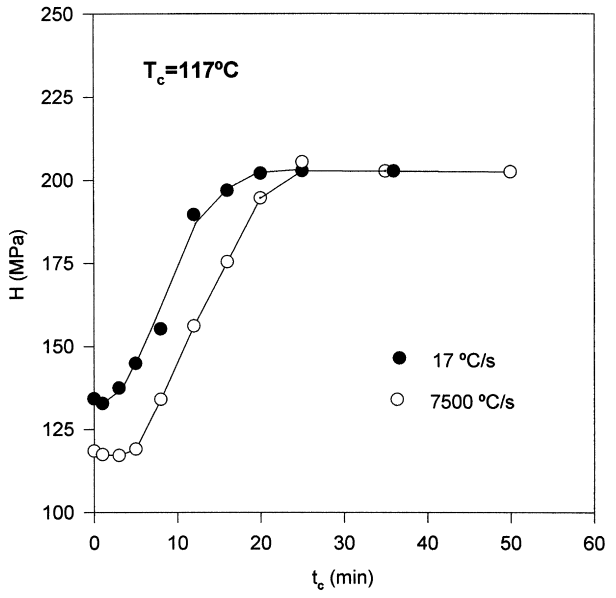

Fig. 6. Variation of H, measured at room temperature, for samples 1 (open circles) and 7 (filled circles) as a function of cold crystallization at 117°C for different cumulative times, t_c.

in poly(butylene terephthalate) [19] and isotactic polypropylene [20].

3.3. Chain ordering of the glassy state

In order to verify the occurrence of possible 'frozen-in' electron density fluctuations induced at different cooling rates, we have recorded the SAXS patterns, using synchrotron radiation, for the amorphous samples 1 and 7. Fig. 5 illustrates the SAXS patterns of these two glassy samples, recorded at room temperature and normalized to the intensity maximum. The intensity difference curve (dotted line and inset of Fig. 5) between the SAXS profiles of samples 7 and 1 is also shown. Although one sees the continuous character of the intensity curve of the individual SAXS profiles, the striking intensity maximum arising from the intensity difference between samples (insert) could be associated to the frozen-in electron density fluctuations from sample 7 with reference to sample 1.

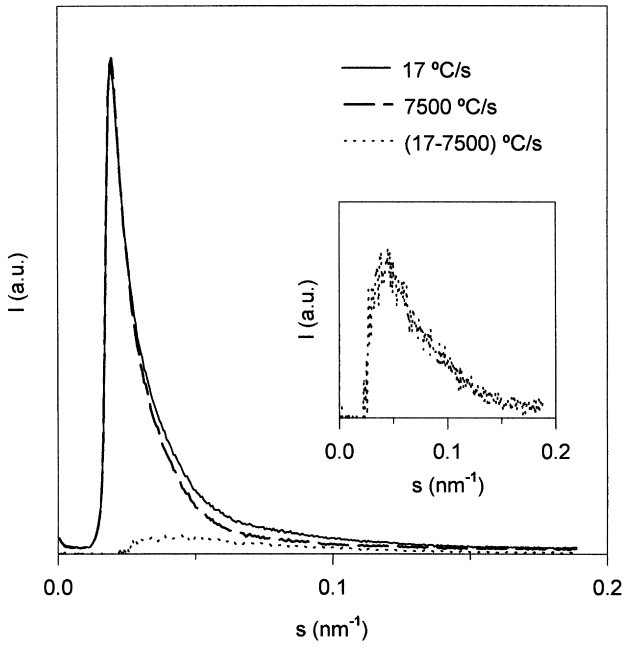

Fig. 5. SAXS intensity profiles obtained at room temperature for samples cooled at 17°C/s (7) and 7500°C/s (1). The intensity difference between the SAXS profiles 7 and 1 (dotted curve and insert) is also shown.

Taking into account that sample preparation was performed by cooling from the melt, it seems plausible to think that the different glassy structures obtained (samples 1–7 of Table 1) should arise because of differences in the heat exchange from PET samples. This idea aimed us to carry out additional experiments to induce embryonic precrystallization states by annealing glassy PET at different times. Indeed, recent results confirm that the time scale for electron density fluctuations during cold crystallization depends on the level of "chain ordering" of the glassy state [21].

3.4. Development of microstructure during cold crystallization

To examine the influence of the initial glassy structure on the cold crystallization of PET, as revealed by H, samples 1 and 7 were again selected. Fig. 6 shows the variation of H, measured at room temperature, as a function of crystallization time at $T_c = 117$°C for these two samples. In both cases a gradual H increase with t_c leading to a final leveling-off after $t_c = 20$–25 min gives rise to final H-values of about

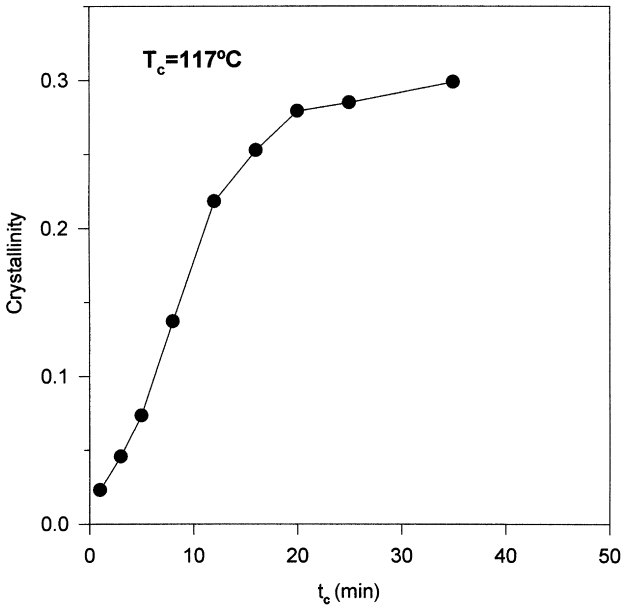

Fig. 7. Variation of degree of crystallinity, α (derived from density) of sample 7 upon isothermal cold crystallization at 117°C for different times.

200 MPa. The results agree well with earlier data for PET samples crystallized at the same temperature [8]. There is, however, a notable *H*-time dependence on the cooling rate. While sample 1 shows an induction period ($t_{ind} \sim 6$ min) before *H* increases, sample 7 having higher initial *H*-values, shows an immediate *H* increase. Beyond t_{ind} both samples present a similar *H* increase with t_c. Sample 7, showing higher *H*-values and larger SAXS intensity (Fig. 5) than sample 1, probably entails "ordered embryonic states" (seeds) which are capable to crystallize more readily as a function of time. On the other hand, sample 1 requires an induction period of a few minutes before the first nuclei appear and develop into crystalline regions responsible for the *H* increase observed. We suggest that the larger induction period detected for sample 1 should be related to the smaller low angle scattering intensity and the smaller *H*-values in relation to sample 7. This induction time difference cannot be explained by differences in equilibrium recovery by the glassy material, which should be much faster at ca 40°C above the glass transition.

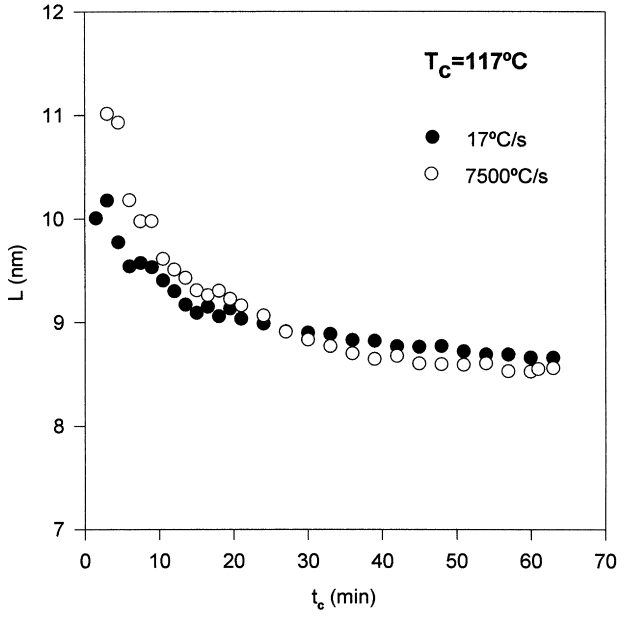

Fig. 8. Variation of the long period measured during isothermal crystallization at 117°C for samples 1 (open circles) and 7 (filled circles).

It is to be noted that after annealing at 117°C for $t_c \simeq 20$ min the primary crystallization process ends and the *H*-values level-off. However, for $t_c > 20$ min (secondary crystallization region), while *H* remains constant the crystallinity shows a further slight increase with t_c (Fig. 7). One may ask, what is the origin for the different behavior between *H* and α in the region of secondary crystallization? An explanation to account for this discrepancy could be the occurrence of a rigid amorphous phase within and in between the spherulites after the second crystallization regime has started. Hence, during primary crystallization the interspherulitic amorphous regions show a hardness value, H_a, which is smaller than the hardness of the crystals, H_c. However, after primary crystallization is completed, the constant *H*-value attained, with a further increase in crystallinity due to secondary crystallization, suggests that H_a should be approximately equal to H_c. Consequently, from the two-phase model ($H = \alpha H_c + (1 - \alpha)H_a$), $H = H_a = H_c = 200$ MPa. If we use the equation for the crystalline hardness [6]:

$$H_c = \frac{H_c^{\infty}}{1 + (b/l_c)} \tag{1}$$

assuming a value for $H_c^{\infty} = 400$ MPa [20] it turns out that $b = l_c$. In previous studies, crystal thickness, l_c values of about 30 Å for PET samples annealed (crystallized) at 117°C have been reported [22]. This should give *b*-values of about 30 Å, in good agreement with data of highly crystalline PET previously reported.

The cold crystallization of the samples 1 and 7 at 117°C has also been investigated, in real time, by simultaneous WAXS and SAXS experiments using synchrotron radiation at HASYLAB. The variation of the long period *L* with the crystallization time has been represented in Fig. 8. For the shorter t_c values sample 1 clearly shows larger *L*-values than sample 7. It seems that during primary crystallization (for $t_c \leq 25$ min) *L* is larger for sample 1 than for sample 7 while for $t_c > 25$ min (secondary crystallization) the *L* values are indistinguishable from each other.

The data concerning the initial development of *L*-values (Fig. 8) seem to be in agreement with the initial *H*-values observed for samples 1 and 7 (Figs. 2 and 3). Indeed, a large long period represents a higher average length between regions of high electron density, i.e. a larger distance between the above mentioned 'embryonic states'.

Consequently, sample 1 with a larger long period than sample 7 should show a smaller volume density of "ordered chain segments" thus giving rise to a smaller hardness value in relation to sample 7.

4. Conclusions

1. The properties and internal structure of glassy PET can be modulated by controlling the cooling rate of molten thin films. Amorphous-PET samples were obtained for cooling rates larger than 4–5°C/s.
2. Amorphous-PET reveals a distinct rise in hardness with decreasing cooling rate which is accompanied by small increasing variations in density as well as in the SAXS intensity.
3. The varying hardness values for the glassy material can be associated to the presence of 'embryonic precrystallization states' which are revealed as an excess of SAXS intensity. The latter is larger the lower the cooling rate.
4. When glassy PET is annealed ($T_c = 117$°C) the samples having the larger induction period prior to crystallization are the ones with the lower initial hardness and scattering intensity values.

Acknowledgements

Grateful acknowledgment is due to the International Joint Research Grant NEDO, Japan and to the DGICYT, Spain (Grant PB94-0049) for the support of this investigation. Resolved measurements of simultaneous SAXS and WAXS during isothermal crystallization of PET at the polymer beam-line A2 were funded by the Program Human Capital and Mobility, Access to Large Installations EC (TMR-Contract ERBFMGECCT950059). Financial support to one of us (S.P.) is acknowledged from the Italian Ministry of Universities (ex 40% quota).

References

[1] Brucato V, Crippa G, Piccarolo S, Titomanlio G. Polym Eng Sci 1991;31:1411.
[2] Piccarolo S, Saiu M, Brucato V, Titomanlio G. J Appl Polym Sci 1992;46:625.
[3] Piccarolo S. J Macromol Sci: Phys B 1992;31(4):501.
[4] Brucato V, Piccarolo S, Titomanlio G. Macromol Symp 1993;68:245.
[5] Brucato V, Piccarolo S, Titomanlio G. Int J Form Processes 1998;1:35.
[6] Baltá Calleja FJ. Trends Polym Sci 1994;2(12):419.
[7] Baltá Calleja FJ, Fakirov S. Trends Polym Sci 1997;5:246.
[8] Santa Cruz C, Baltá Calleja FJ, Zachmann HG, Stribeck N, Asano T. J Polym Sci: Polym Phys B 1991;29:819.
[9] Ania F, Martínez-Salazar J, Baltá Calleja FJ. J Mater Sci 1989;24:2934.
[10] Baltá Calleja FJ, Santa Cruz C, Asano T. J Polym Sci: Polym Phys 1993;31:557.
[11] Baltá Calleja FJ, Baranowska J, Rueda DR, Bayer RK. J Mater Sci 1993;28:6074.
[12] Brucato V, Piccarolo S, Titomanlio G. Analysis of non-isothermal crystallization kinetics of PET, European PPS Meeting, 1995. p. 5–30, Stuttgart, 26 September.
[13] Fakirov S, Fischer EW, Schmidt R. Makromol Chem 1975;176:2459.
[14] Gehrke R, Zachmann HG. Makromol Chem 1981;182:627.
[15] Baltá Calleja FJ, Martínez Salazar J, Rueda DR. Encyclopedia of polymer science engineering, 6. New York: Wiley-Interscience, 1986. p. 614.
[16] Struik LCE. Physical aging in amorphous polymers and other materials, Amsterdam: Elsevier, 1978.
[17] Imai M, Mori K, Mizukami T, Kaji K, Kanaya T. Polymer 1992;33:4451.
[18] Ezquerra TA, López Cabarcos E, Hsiao BS, Baltá Calleja FJ. Phys Rev E 1996;54:989.
[19] Hsiao BS, Wang Z, Yeh F, Gao Y, Sheth KC. Polymer 1998;40:3515.
[20] Terril NJ, Fairclough PA, Towns-Andrews E, Komanschek BU, Young RJ, Ryan AJ. Polym Commun 1998;39:2381.
[21] García MC, Rueda DR, Baltá Calleja FJ. Polym J 1999;9:806.
[22] Baltá Calleja FJ, Öhm O, Bayer RK. Polymer 1994;35:4775.